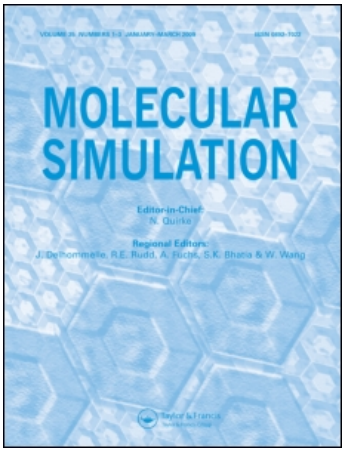

Molecular Simulation
Publication details, including instructions for authors and subscription information:
http://www.informaworld.com/smpp/title~content=t713644482

Simulation study of ammonia adsorption on graphitized carbon black

G. R. Birkett[a]; D. D. Do[a]
[a] Department of Chemical Engineering, University of Queensland, Brisbane, QLD, Australia

To cite this Article Birkett, G. R. and Do, D. D.(2006) 'Simulation study of ammonia adsorption on graphitized carbon black', Molecular Simulation, 32: 7, 523 — 537
To link to this Article: DOI: 10.1080/08927020600622030
URL: http://dx.doi.org/10.1080/08927020600622030

Molecular Simulation, Vol. 32, No. 7, 15 June 2006, 523–537

Taylor & Francis
Taylor & Francis Group

Simulation study of ammonia adsorption on graphitized carbon black

G. R. BIRKETT and D. D. DO*

Department of Chemical Engineering, University of Queensland, St Lucia, Brisbane, QLD 4072, Australia

(Received November 2005; in final form March 2006)

GCMC simulations are applied to the adsorption of sub-critical ammonia on graphitized carbon black at 240 K. The carbon black was modelled both with and without carbonyl functional groups. Large differences are seen between the amount adsorbed for different carbonyl configurations at low pressure ($P < 10$ kPa). Once a single layer is formed on the carbon black, the adsorption behaviour is similar between the model surfaces with and without functional groups. Simulation isotherms are qualitatively similar to the few experimental isotherms available in the literature for ammonia on highly graphitized carbon black. The mode of adsorption up to monolayer coverage is exhaustively shown to be two-dimensional clustering using various techniques. A comparison between experiment and simulation isosteric heats shows that a surface without functional groups cannot reproduce the experimental isosteric heats of adsorption, even comparing with the experimental results of carbon black heat treated at 3373 K. The addition of carbonyls produces isosteric heats with similar features to those in the literature if the separation between the carbonyls is small.

Keywords: Molecular simulation; Ammonia; Adsorption; Carbon black

1. Introduction

The study of adsorption is a mature science with a large body of experimental work and theoretical study behind it. Currently, the predominant field in the theoretical study of adsorption phenomena is in molecular simulation. The potential of molecular simulation to offer insight into molecular scale behaviour has been apparent since the very first simulation performed by Metropolis *et al.* [1]. Since this time, the popularity of molecular simulations has increased with increased computing power and improved methods with adsorption being just one field where it is applied.

Carbon adsorbents represent a major sub-category of adsorbents. Within the family of carbon adsorbents there is a wide range of characteristics from the complex structure of activated carbons to graphite and well defined nanotubes. Molecular simulation provides an appealingly direct way of understanding adsorption behaviour. In principle, if one is able to describe the interaction between fluid particles and that between a fluid particle and the adsorbent, it is possible to predict the amount adsorbed and the state of adsorbed molecules. This has been done with a large degree of success with non-polar molecules. This has allowed for improved description of both pore size distributions and adsorption isotherms. Such confidence in adsorption simulations has yet to translate to strongly associating fluids. Of the family of strongly associating fluids, water is the most important and widely studied. However, there are many other important fluids that fall into this category of which ammonia is one. In addition to being industrially important, ammonia is interesting because it falls between non-polar fluids and water in the relative importance of coulombic to dispersive interactions. So the factors that effect ammonia adsorption are similar to those of water. So any model used to describe the adsorption of water on carbon black should be able to also describe the major features of ammonia adsorption. This paper will present the results of a simulation study of ammonia on a simple model of carbon black and compare them with experimental results from the literature.

*Corresponding author. Tel: 61 7 3365 4154. Fax: 61 7 3365 2789. Email: duongd@cheque.uq.edu.au

Molecular Simulation
ISSN 0892-7022 print/ISSN 1029-0435 online © 2006 Taylor & Francis
http://www.tandf.co.uk/journals
DOI: 10.1080/08927020600622030

2. Potential models

2.1 Ammonia potential model

The model for ammonia used in the simulations is that proposed by Kristof *et al.* [2]. This is a four site model of ammonia with a site for each of the nitrogen and hydrogen atoms. There is a single Lennard Jones site located at the nitrogen atom. There are four partial charges with three positive charges located at the hydrogen atoms and a single negative charge located at the nitrogen atom. The potential energy between two ammonia molecules is given by equation 1.

$$u_{ij} = \frac{1}{2}\sum_{\alpha=1}^{A}\sum_{\beta=1}^{B}\frac{q_i^{\alpha}q_j^{\beta}}{4\pi\varepsilon_0 r_{ij}^{\alpha\beta}} + 4\varepsilon_{ff}\left[\left(\frac{\sigma_{ff}}{r_{ij}}\right)^{12} - \left(\frac{\sigma_{ff}}{r_{ij}}\right)^{6}\right] \quad (1)$$

where u_{ij} is the interaction energy between ammonia molecules i and j, σ_{ff} is the nitrogen collision diameter, r_{ij} is the separation between nitrogen sites, ε_{ff} is the nitrogen well depth, $r_{ij}^{\alpha\beta}$ is the separation between the α charge on molecule i and the β charge on molecule j having charges q_i^{α} and q_j^{β}, respectively, $A = B = 4$ is the number of charges on an ammonia molecule and ε_0 is the permittivity of a vacuum. The parameters of the ammonia model were optimised to fit vapour liquid co-existence data above 281 K by its authors [2]. The model is characterized by ε and σ, the Lennard Jones well depth and collision diameter of the nitrogen, q^- and q^+, the partial charges of the nitrogen and hydrogen atoms, R_{NH}, the N–H bond length, and by θ_{HNH}, the angle formed between two N–H bonds. The values of the molecular parameters for the ammonia model are given in table 1.

The vapour pressure of this ammonia model at 240 K has been determined by GEMC [3] as 107 kPa (± 19 kPa). This compares to the experimental vapour pressure of 102 kPa for ammonia. So these parameters produce a good approximation of the vapour pressure at this temperature. This is outside the range of the optimisation performed by its authors [2] of 281 K to the critical point but appears to be the most suitable potential model available in the literature.

2.2 Carbon black

The simulation cell is bound in the z-direction by the walls of a slit pore. Only one of the walls of the pore has an attractive interaction with the fluid molecules. This pore wall interacts with a fluid molecule according to the Steele 10-4-3 potential [4] given by equation 2.

$$u_i(z_i) = 2\pi\rho_s\varepsilon_{fs}\sigma_{fs}^2\Delta\left[\frac{2}{5}\left(\frac{\sigma_{fs}}{z_i}\right)^{10} - \left(\frac{\sigma_{fs}}{z_i}\right)^{4} - \left(\frac{\sigma_{fs}^4}{3\Delta(z_i + 0.61\Delta)^3}\right)\right] \quad (2)$$

Table 1. Molecular parameters of ammonia model.

ε/k_b (K)	σ(nm)	q^- (e)	q^+ (e)	R_{NH} (nm)	θ_{HNH} (deg)
170	0.3385	−1.035	0.3385	0.10124	106.68

Table 2. Molecular parameters of carbon surface used in the Steele 10-4-3 equation.

σ_{ss}(nm)	ε_{ss}/k_b(K)	ρ_s(nm^{-3})	Δ(nm)
0.34	28.0	114	0.335

where $u_i(z_i)$ is the interaction between an ammonia molecule, i, and the wall with its nitrogen atom a distance z_i from the wall, σ_{fs} is the fluid–solid collision diameter, ε_{fs} is the fluid–solid well depth, ρ_s is the graphite's carbon density and Δ is the separation between graphite layers. The values of σ_{fs} and ε_{fs} are given by Lorentz-Berthelot mixing rules in equations 3 and 4.

$$\varepsilon_{fs} = \sqrt{\varepsilon_{ff}\varepsilon_{ss}} \quad (3)$$

$$\sigma_{fs} = 0.5\left(\sigma_{ff} + \sigma_{ss}\right). \quad (4)$$

The molecular parameters for the carbon wall Steele potential are given in table 2.

The opposing wall has no attractive term and has only an effectively infinite repulsion for molecules that cross the pore wall. The simulation cell is repeated periodically in the x and y directions to approximate an infinite pore. The model pore has a width of 5.0 nm and a length in the simulation cell of 7.5 nm. A simulation cell length 1.5 times the pore width has been observed to be sufficient by Jorge and Seaton [5] to avoid observable finite size effects and this has been the experience of the authors as well. A pore width of 5.0 nm allows a good approximation of carbon black with the opposing hard wall having no observable effect on the adsorption at the Steele potential surface until many layers are formed.

2.3 Carbonyl functional groups

The only type of functional group considered in this study is carbonyl. This is modelled with a single LJ site at the oxygen at a distance, R_{CO}, perpendicular to the carbon surface, a positive charge on the surface and a negative charge at the oxygen. The parameters for the carbonyl group are taken from the OPLS potential model for amino acids [6] and are given in table 3.

The configuration of functional groups has previously been observed to strongly affect the adsorption behaviour of water [7]. This is expected to be the case for ammonia as well. It was decided to use configurations involving either a closely associated group(s) of five carbonyls or evenly distributed carbonyl groups. The three types of carbonyl configurations are shown in figure 1.

The interaction between ammonia molecules and the carbonyls is given by equation 1 with $A = 2$ and the LJ

Table 3. Molecular parameters of carbonyl group.

ε/k_b(K)	σ(nm)	q^-(e)	q^+(e)	R_{CO}(nm)
105.8	0.296	−0.5	0.5	0.1233

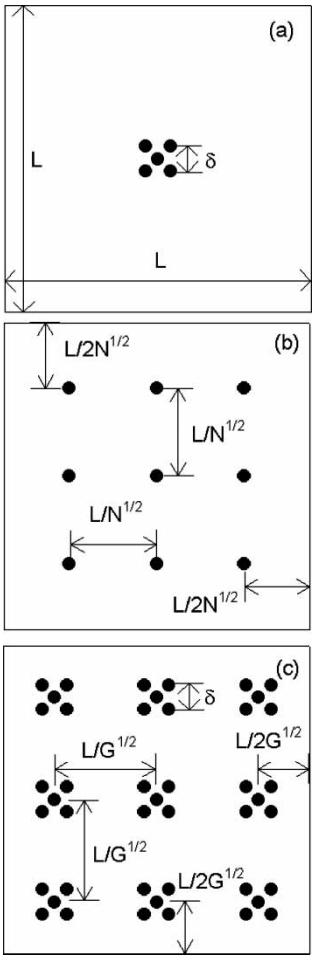

Figure 1. Configurations of carbonyls (●) on the bottom plane of the pore: (a) group of five carbonyls located at the centre of the pore wall; (b) evenly spaced single carbonyls; and (c) evenly spaced groups of five carbonyls. δ = the characteristic separation of a group of five carbonyls, L = simulation cell box length in x and y axis, N = the number of evenly spaced carbonyls and G = the number of groups of five carbonyls.

parameters given by the combination of their respective LJ parameters using the Lorentz-Berthelot mixing rule (equations 3 and 4). Carbonyls, as opposed to other functional groups, were chosen for their simplicity and that carbonyls represent a large percentage of the functional groups on carbon blacks treated at high temperatures [8,9]. The simplicity of carbonyls offers a very small saving in computational cost compared with hydroxyl or carboxyl groups but more importantly, reduces the parameters that can be adjusted. Carbonyls can only be adjusted by their positions whereas hydroxyl and carboxyl groups must have their orientation specified. This combined with the fact that comparison is being made between simulation and experiments on carbon blacks heat treated at high temperatures makes carbonyl a good choice for this preliminary study.

3. Simulation methodology

Monte Carlo simulations were conducted using the standard GCMC ensemble [10]. The chemical potentials used in the simulations were the ideal chemical potential of the pressures reported. Simulations were conducted at 240 K at pressures from 0.01 to 100 kPa. Each simulation isotherm point was conducted over a number sub-ensembles consisting of 1000 cycles each. Each cycle consisted of (on average) 200 moves and varying (but equal) numbers of insertions and deletions. The number of insertions was set to give an acceptance rate of approximately four insertions per cycles. A move consisted of either a translation or a rotation (about one randomly selected axis) with equal probability. Maximum translations and rotations were adjusted separately to give an approximate acceptance of 50% of moves. Performing translation and rotation moves separately was found to reach equilibrium faster than performing a combined move. Once ten sub-ensembles had been performed a running average of the number of ammonia molecules in the previous ten sub-ensembles was recorded, $\langle N_{10} \rangle$. Once $\langle N_{10} \rangle$ starts oscillating about the same value, the simulation is considered to be at equilibrium. From this point ten more sub-ensembles are performed. It is the final ten sub-ensembles which comprise the results reported. Once an isotherm point is completed, its final configuration is used as the initial configuration of the next isotherm point, mimicking the experimental adsorption procedure.

No long-range corrections were used for either dispersion (LJ) or electrostatic interactions. LJ interactions were cut at a cylindrical cut-off in the x-y plane at a distance R_c. Coulomb interactions were cut on a molecular basis based upon the nitrogen position of the ammonia molecule. So if two molecules satisfied the LJ cut-off criteria with their nitrogen atoms, all Coulomb interactions were counted between the particles even if some charge separations were greater than R_c in the x-y plane. Cut-offs on an atomistic charge-charge basis would lead to spuriously high interactions between non-neutrally charged molecules. The same cut-offs were applied to the interactions of ammonia molecules with carbonyl sites. For comparison with experiments conducted in the literature, the isosteric heat was calculated for all simulations. The isosteric heat was calculated using equations 5 [11].

$$q_{st} \cong \frac{\langle NU \rangle - \langle N \rangle \langle U \rangle}{\langle N^2 \rangle - \langle N \rangle \langle U \rangle} + kT. \tag{5}$$

The first term in equation 5 can also be split into the different contributions to the system potential energy U. The three contributions to the potential energy are the fluid–fluid interactions, the fluid-surface interactions and the fluid-functional interactions. Replacing U in equation 5 with one of these contributions to the potential, and discounting the second term, will give its contribution to the isosteric heat.

4. Results

The first series of results presented in figure 2 are for simulations completed at 240 K on a surface with no carbonyls and with a cluster of five carbonyls at the centre

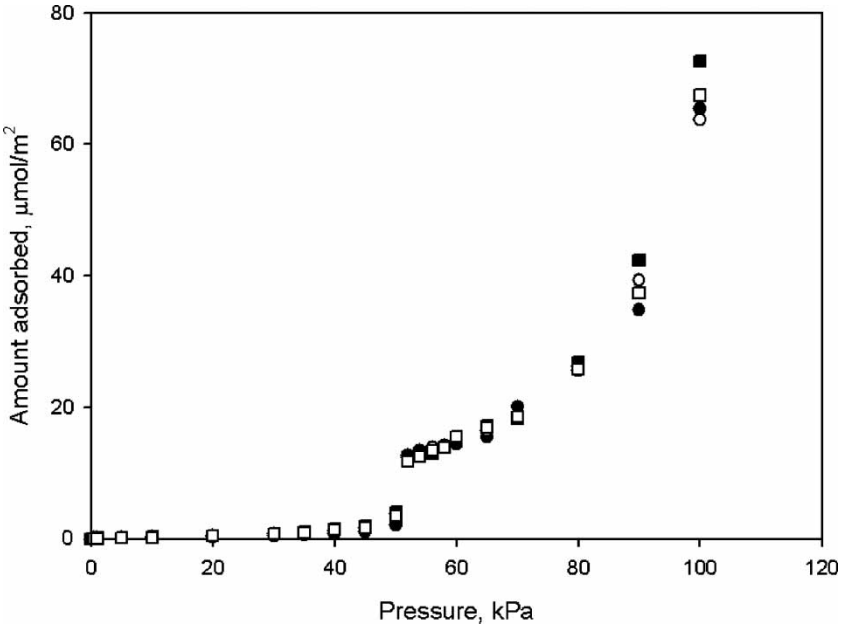

Figure 2. Simulation results for the adsorption of ammonia at 240 K on carbon black with no carbonyls (filled circles) and with five carbonyls located at the centre with separations, δ, of 0.15 nm (empty circles), 0.3 nm (filled squares) and 0.6 nm (empty squares).

with characteristic separations, δ, of 0.15, 0.3 and 0.6 nm (referring to figure 1(a)).

The isotherms in figure 2 show some interesting behaviour. At pressures less than 52 kPa, the adsorption is relatively low. At 52 kPa the amount adsorbed undergoes a step change. This step change is the condensing of a monolayer (approximately). This aspect will be discussed further later in this paper. At increasing pressures from 52 kPa the amount adsorbed increases slowly before increasing in an exponential manner. This broad description of the behaviour is the same for all the centre configurations of five carbonyls presented in figure 2. Adsorption experiments for ammonia on carbon black have been reported by Spencer *et al.* [12] and Avgul and Kiselev [13]. The results from Spencer *et al.* are from experiments on Sterling MT, a highly graphitized carbon black heat treated at 3373 K, at 194.15 K. The results from Avgul and Kiselev are for adsorption on a similarly graphitized carbon black at 195.15 K. Their results are presented in figure 3 together with the simulation results

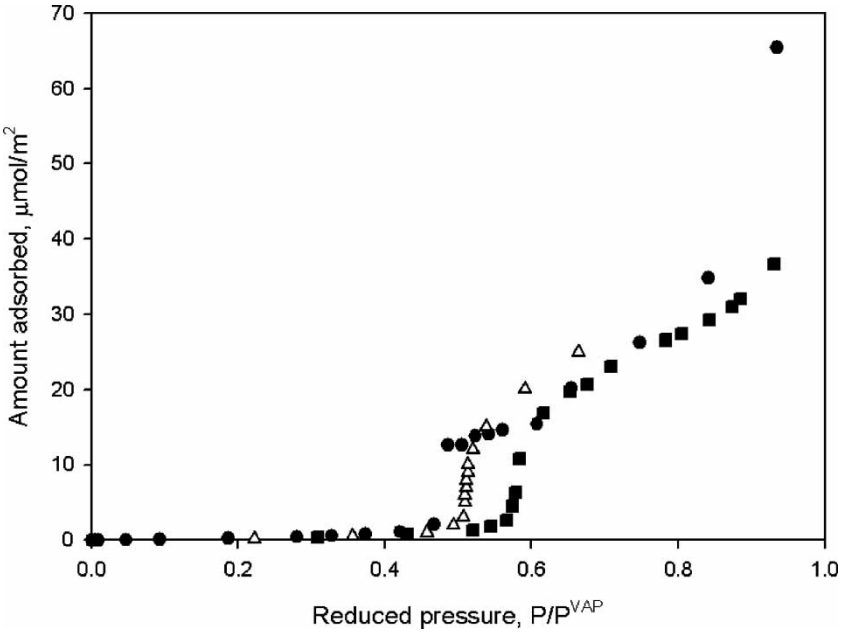

Figure 3. Experimental adsorption isotherms for ammonia at 194.15 K (empty triangles) and 195.15 K (filled triangles), from Spencer *et al.* [12] and Avgul and Kiselev [13], respectively, on highly graphitized carbon blacks together with the isotherm from a simulation at 240 K on a graphite surface with no functional groups (filled circles). The amount adsorbed is plotted versus the pressure reduced by the experimental vapour pressure, for the experimental data, and the ideal simulation pressure reduced by the ammonia models vapour pressure at 240 K for the simulation results.

for a surface with no functional groups. The experimental results have their pressure reduced by the experimental vapour pressure and the simulation isotherm, by the ammonia model's vapour pressure. The simulation isotherm is at a temperature of 240 K.

The major features of the experimental isotherms in figure 3 are qualitatively similar to those of the simulation isotherms. Both give low initial adsorption followed by a sharp uptake. Following this sharp uptake the isotherms go through a point of inflection. After this the amount adsorbed again increases more sharply with pressure. This is followed to higher surface coverage in figure 2 and the simulation isotherm in figure 3 and shows no sign of a limit. So whilst the qualitative features of the experimental isotherms are also seen in the simulation isotherms, the quantitative comparison is not good. This, however, should not necessarily be so considering the differences in temperature. The clearest difference is the reduced pressure at which the sharp uptake occurs. This happens at $P/P^{\mathrm{VAP}} \approx 0.47$ for the simulation isotherm and $P/P^{\mathrm{VAP}} \approx 0.58$ and 0.51 for the isotherms from Spencer *et al.* [12] and Avgul and Kiselev [13], respectively. This seems reasonable for two reasons. The first is that the agreement between the experiments is not good meaning there is some doubt about the uptake pressure. The second is the difference in the temperatures that the experiments, 194.15 and 195.15 K, and the simulations, 240 K, were performed. In a study of ammonia adsorption on a similar (but slightly less graphitized) carbon black, Dell and Beebe [14] showed that as temperature is increased the initial sharp increase in the amount of ammonia adsorbed occurs at lower relative pressures. They found the relative pressure at which the initial sharp increase occurred decreased by 0.06 when the temperature was changed from 194.35 to 236.85 K. This is greater than the difference between simulation and experiment. Undoubtedly, there would be differences due to the ammonia and/or graphite model too. No attempt has been made to optimize this because of the lack of reliable data. The next major difference is the much sharper inflection point for the simulation compared with the experimental isotherms. The simulation isotherm is very flat after the inflection point whereas the experiment data certainly does not flatten to the same extent. This could possibly be due to the greater heterogeneity of the real surface compared to the idealised one used in the simulation. The quantitative differences are to be expected and will not be resolved in this paper. It is not the objective of this paper to fit experimental data exactly but rather to demonstrate the mode of ammonia adsorption on carbon black. So while the qualitative agreement is good and the quantitative differences appear to be not too significant, it is reasonable that to assume that the simulation adsorption is occurring by the same mechanism as in the experiment.

The difference between the isotherms of different carbonyl configurations is not clearly seen in figure 2. Differences between the adsorption isotherms of the different carbonyl configurations can better be seen at pressure less than 52 kPa. Figure 4 presents the results of figure 2 over the range of 0–50 kPa to show increased detail in this range.

Figure 4 shows that whilst the isotherms of the different carbonyl configurations appear very similar over the pressure range of 0–100 kPa, they are quite different in the range of 0–50 kPa. The adsorption at pressures less than 1.1 kPa (inset in figure 4) is favoured by more closely packed carbonyls with a configuration of no carbonyls giving the lowest adsorption. The isotherms of 0.15 and

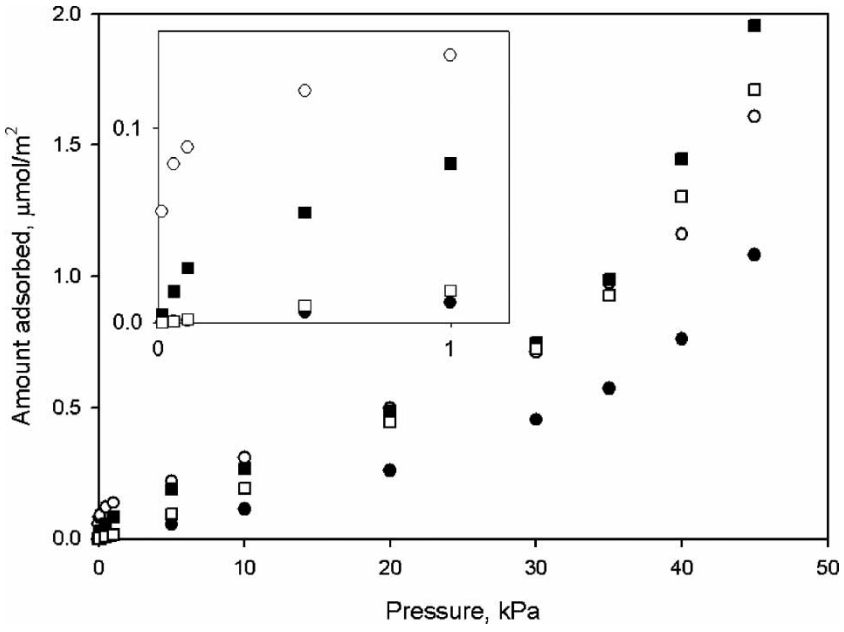

Figure 4. Simulation results for the adsorption of ammonia at 240 K on carbon black for pressures less than 50 kPa. Symbols are the same as figure 2. Inset shows the same results for pressures less than 1.1 kPa.

0.3 nm separated carbonyls are very similar in shape with an initial sharp pick-up giving the isotherm a type-II appearance in this pressure range. The 0.15 nm separation in particular has a very sharp pick-up with significant adsorption at the lowest pressure of 0.01 kPa. In contrast the carbon black with no carbonyls and the carbonyls separated by 0.6 nm having isotherms closer to type III with no steep initial pick-up in the amount adsorbed. At pressures greater than 10 kPa all isotherms show a similar exponential increase in the amount adsorbed. All three carbonyl configurations give similar amounts adsorbed with the carbonyl free surface giving significantly less. Such differences in the adsorption isotherms would suggest differences in the isosteric heats for the different arrangements. The isosteric heats for the adsorption isotherms in figure 2 are presented in figure 5.

Figure 5 shows a clear difference between the isosteric heats for the different carbonyl configurations. For carbonyl separations of 0.15 and 0.3 nm, the isosteric heat is initially much greater than the heat of vaporisation. As the amount adsorbed increases, the heat of adsorption decreases and becomes less than the heat of vaporisation. The isosteric heat then goes through a minimum before returning to a value close to the heat of vaporisation. The isosteric heat for both the carbon black with the 0.6 nm separated carbonyls and with no carbonyls is initially less than the heat of vaporisation. As the amount adsorbed increases, the isosteric heat also increases until it is approximately equal to the heat of vaporisation. It is interesting to note that the isosteric heat for all isotherms increases in much the same way once the amount adsorbed is greater than 0.5 μmol/m^2 suggesting that the mode of adsorption may be similar for all four configurations past this point. The difference in the heats of adsorption must be due to the carbonyl groups and their configurations. This can be shown clearly by splitting the isosteric heat into its contributions from fluid–fluid, fluid–solid and fluid-functional interactions. These contributions to the isosteric heat are shown in figure 6 for a surface with no functional groups and one with five carbonyls and $\delta = 0.3$ nm.

It can be seen in figure 6 that the fluid–fluid and fluid–solid contributions to the isosteric heat are almost identical for the surfaces with and without the carbonyl groups. The difference in the total isosteric heat comes solely from the interaction of ammonia with the carbonyl groups. The contribution of the carbonyl groups to the isosteric heat quickly decays to zero giving nearly identical isosteric heats for the two surfaces beyond 0.5 μmol/m^2. The fluid–fluid contributions rise to a maximum giving an isosteric heat approximately equal to the ammonia models heat of vaporisation at high coverage. The contribution from fluid–solid interactions remains essentially constant until the monolayer is formed. This suggests an absence of three-dimensional clustering in the adsorption. Once the monolayer is formed, its contribution monotonically decreases to eventually become insignificant. The same authors who obtained the results in figure 3, Spencer *et al.*

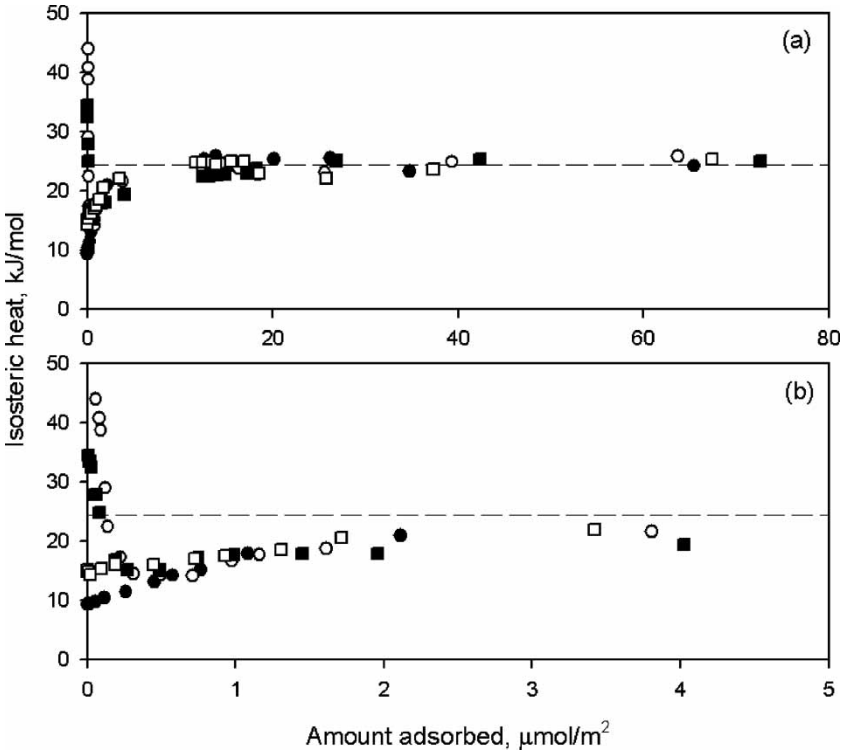

Figure 5. Isosteric heats of adsorption for ammonia on carbon black from simulation. Symbols have the same meaning as figure 2. The horizontal dashed lined corresponds to the enthalpy of vaporisation for model ammonia from GEMC. Figures (a) and (b) differ only in the scale of the amount adsorbed.

[12] and Avgul and Kiselev [13], also calculated the isosteric heat for the adsorption of ammonia on highly graphitized carbon black. Their results are presented in figure 7.

The isosteric heat in figure 7 follows some general trends. Initially, it is greater than the heat of vaporisation, dips to a minimum and increases again. This has been observed in studies of other graphitized carbon blacks also [14,15]. These are similar trends to those seen from the simulations in figure 5 with five carbonyls separated by 0.15 and 0.3 nm. The clear differences between the isosteric heats from these simulations and the ones in figure 7 are that the experimental isosteric heats never drop below the heat of vaporisation in figure 6 and that the minimums in figure 5 are much sharper than the minimums in figure 7. The sharpness of the minimum may again be explained as the difference between a real heterogeneous surface and an ideal model surface. The reason for the minimum in figure 5 being significantly less than the heat of vaporisation is less clear. There has been an experimental observation for isosteric heat lower than the heat of vaporisation [15] but it is not to the same extent as in figure 5. Although these differences are significant, it is clear that the isosteric heat of the carbon black with carbonyls separated by 0.15 and 0.3 nm is in better qualitative agreement with experiment than with carbonyls separated by 0.6 nm or with no carbonyls which rise from a minimum at zero coverage. To better understand the mechanism of adsorption it is possible to look at the distributions of ammonia in the pore. The local pore density as a function of distance from the graphite surface was calculated using equation 6

$$\rho_z = \frac{\langle \Delta N_{z+\Delta z} \rangle}{L_{\text{box}}^2 \Delta z} \tag{6}$$

where ρ_z is the local density calculated as a function of z only, $\langle \Delta N_{z+\Delta z} \rangle$ is the ensemble number of particles in the region from z to $z + \Delta z$. The local density, ρ_z, was measured using segments, Δz, equal to 0.01 nm. Figure 8 shows the local density versus distance from the surface for several pressures for a simulation with five carbonyls and $\delta = 0.3$ nm.

Figure 8 shows that the monolayer density increases monotonically from 1 to 50 kPa and dominates the adsorption. The second layer is discernable from 20 kPa but is at least an order of magnitude less in its density than the first layer. The increase in pressure from 50 to 52 kPa results in a sudden increase in the monolayer, and second layer, density. The suddenness of this transition seems to be what could almost be considered a monolayer condensation. Once this fairly complete monolayer is formed it undergoes only small increases in density but the increase in the amount adsorbed from this point on comes mostly from the formation of additional layers. At the

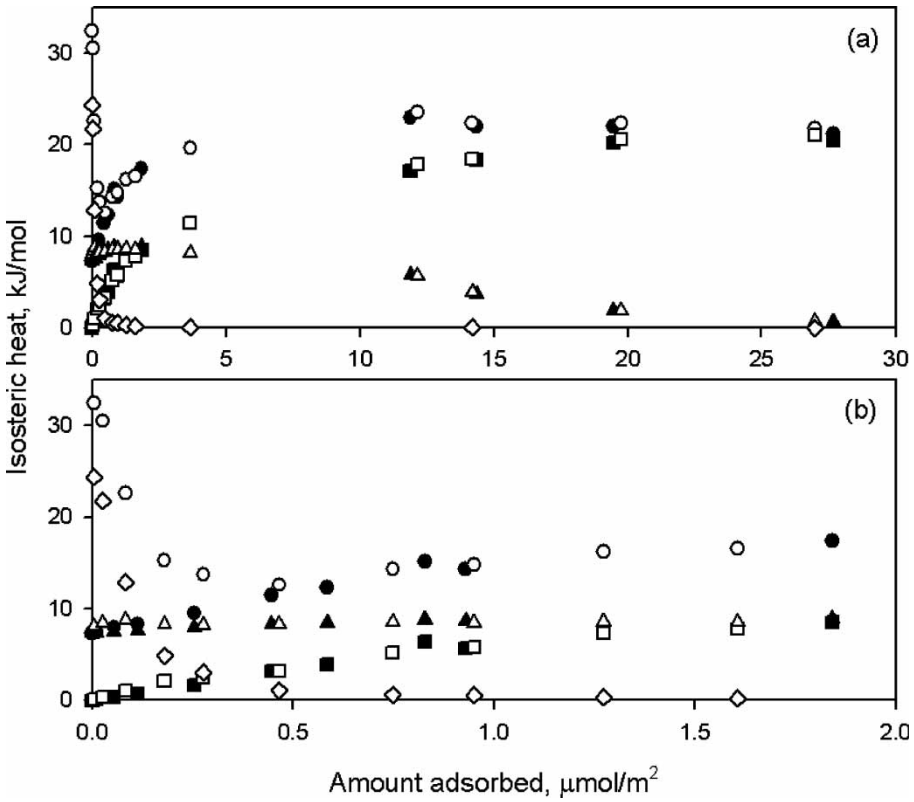

Figure 6. Simulation isosteric heats split into its contributions: total isosteric heat less the second term in equation 5 (circles), due to fluid–fluid interactions (squares), due to fluid solid interactions (triangles) and due to fluid-functional interactions (diamonds). Empty symbols denote the surface with five carbonyls and $\delta = 0.3$ nm and the filled symbols denote the surface with no carbonyls. Plots (a) and (b) differ only in the scale of the amount adsorbed.

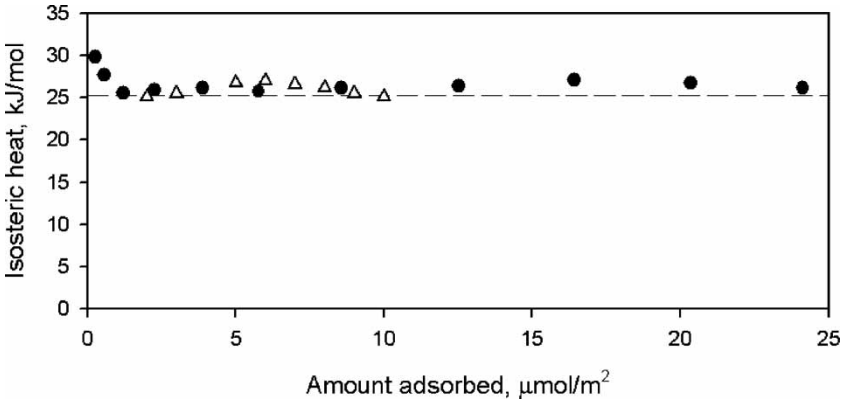

Figure 7. Experimental isosteric heats of adsorption for ammonia on highly graphitized carbon black at 194.15 K (filled circles) and 195.15 K (empty triangles) from Spencer *et al.* [12] and Avgul and Kiselev [13], respectively. Horizontal dashed line is the experimental heat of vaporisation at 195.15 K.

maximum pressure of the simulations, 100 kPa, the first four layers are quite well defined. Beyond this the layers become less distinct and approach the saturated liquid density of 40.5 kmol/m^3 (from GEMC). The behaviour in figure 8 can be compared against a surface with no functional groups which is presented in an identical fashion in figure 9.

There is little difference between the results in figures 8 and 9. The main difference exists in the density of the first layer which is greater for the surface with carbonyls than the surface without for all pressures up to 50 kPa. Even though the adsorption is greater for the surface with carbonyls in figure 8 there is very little adsorption beyond the first layer until there is condensation in the first layer. This suggests that there is little clustering occurring outside of the first layer. So if ammonia molecules are associating before the first layer condenses, they must be doing so in essentially two-dimensional structures. This would agree with the observations of isosteric heat in figures 5 and 6. Another way of investigating this is to look at the two-dimensional radial distribution of the ammonia from the centre (in the *x*-*y* plane) of the pore. The surface radial distribution is calculated using equation 7

$$\zeta_r = \frac{\langle \Delta N_{r+\Delta r} \rangle}{\pi(r+\Delta r)^2 - \pi r^2} \tag{7}$$

where ζ_r is the surface density at a distance, r, from the centre of the pore in the *x*-*y* plane and $\langle \Delta N_{r+\Delta r} \rangle$ is the ensemble number of particles in the region from r to $r + \Delta r$. For the *x*-*y* distributions presented Δr has been set to 0.02 nm. Now the *x*-*y* distribution for the configuration of five carbonyls at the centre of the pore with $\delta = 0.3$ nm is given in figure 10.

Figure 10 shows that at pressures less than 52 kPa there is clearly a higher surface density surrounding and upon

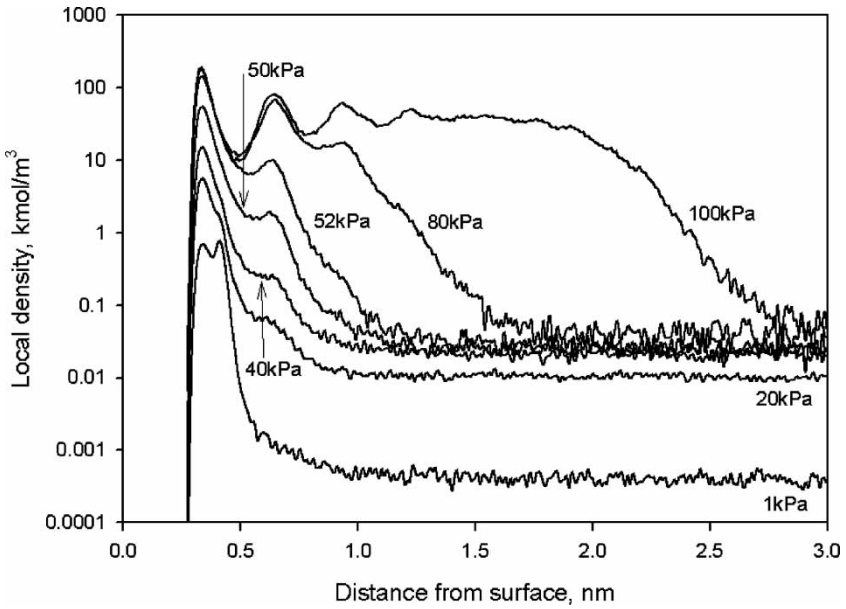

Figure 8. Local density versus distance from graphite surface for several pressures. Results are from a simulation with five centre configured carbonyls with $\delta = 0.3$ nm. Local density is calculated using equation 6.

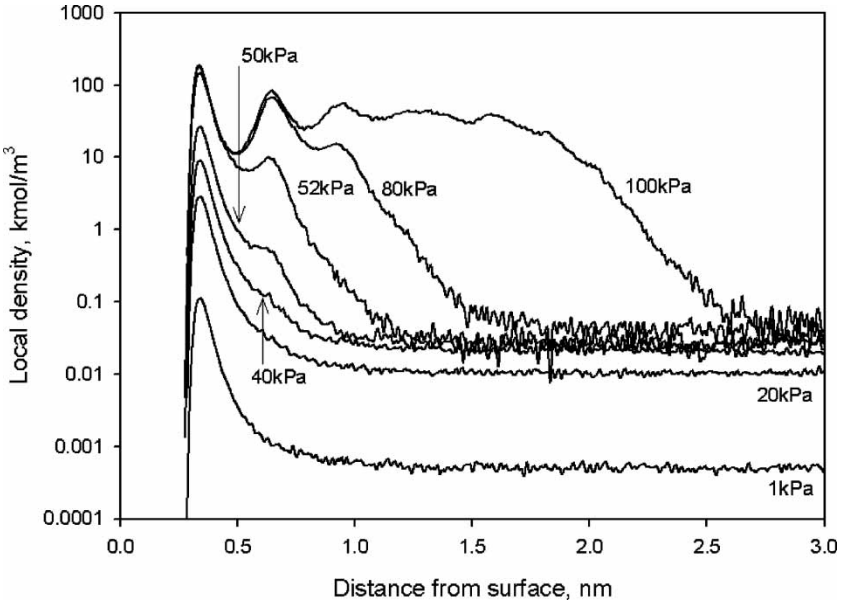

Figure 9. Local density versus distance from graphite surface for several pressures. Results are from a simulation with no carbonyls. Local density is calculated using equation 6.

the carbonyls at the centre of the pore. However the surface density around the carbonyls, up to 0.5 nm, is established at a very low pressure and increases very little as pressure is increased beyond 10 kPa. This shows that no three-dimensional cluster is being formed about the carbonyls. So the adsorption at the remainder of the surface is more important than at the carbonyls beyond 10 kPa. The surface density increases for all radial distances and not just at spreading distances from the carbonyls at the centre. This suggests that two-dimensional ammonia structures are formed about the carbonyls and the associated ammonia molecules and also independently at distant points on the surface. This mode of adsorption would be in agreement with the heats of adsorption in figure 6(b) where the fluid-functional contribution to the isosteric heat after initially being dominant drops to almost zero beyond a surface coverage of 0.5 μmol/m^2. From this point on both configurations in figure 6(b) have the same heat of adsorption. This is in agreement with both having the same mechanism of adsorption. A final way of confirming this mode of adsorption is to look at single configurations from the simulations. Whilst not as rigorous as ensemble distributions, since they show only one configuration of the millions sampled, it is a useful way of visualising what is happening. Simulation snapshots are shown in figure 11

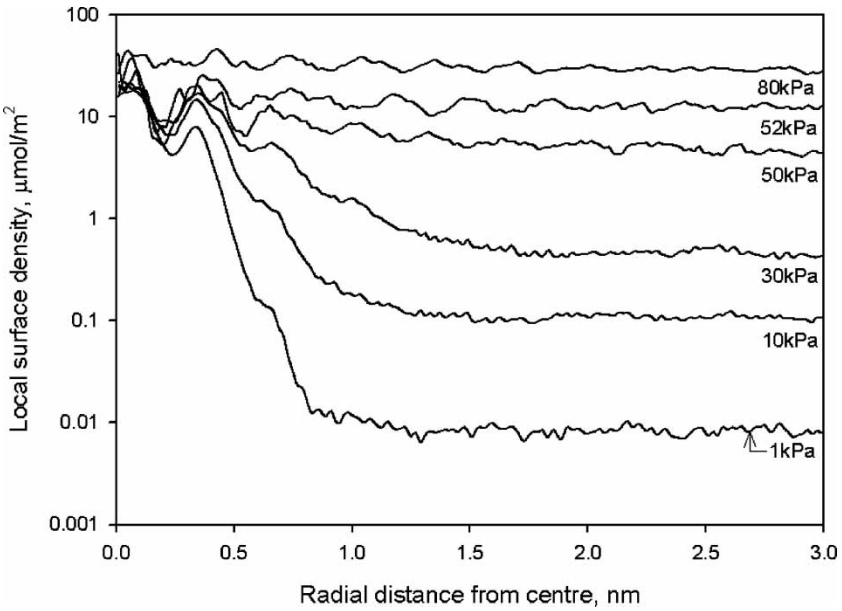

Figure 10. Local surface density versus radial distance from the centre of the pore for several pressures. Results are from a simulation with five carbonyls grouped at the centre of the pore and $\delta = 0.3$ nm. Local surface density is calculated using equation 7.

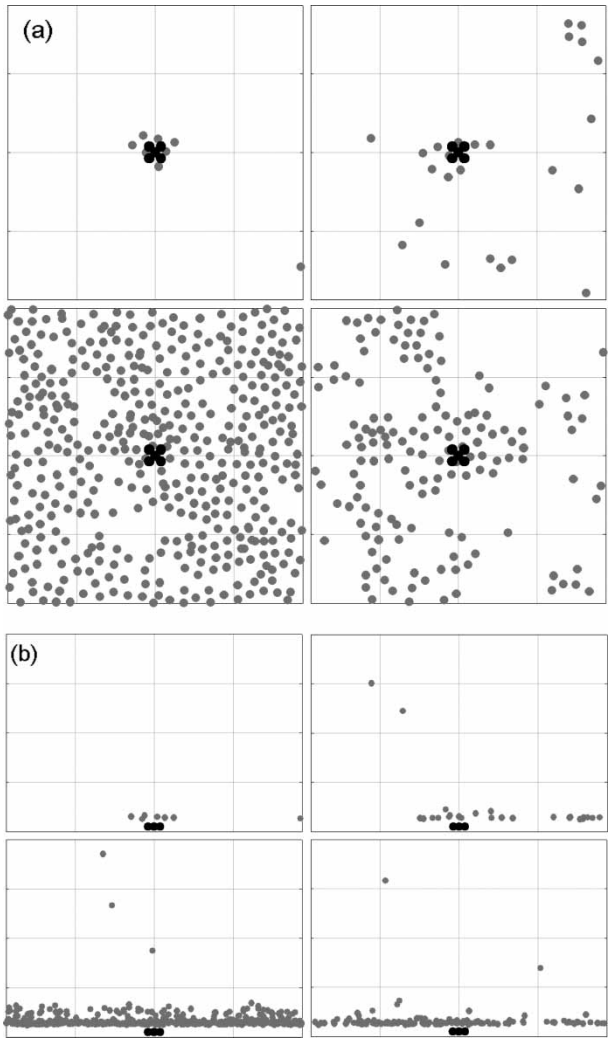

Figure 11. Snapshot of ammonia positions (shown as a single site equivalent to the position of the nitrogen atom with gray filled circles) at equilibrium for a simulation with five carbonyls with $\delta = 0.3$ nm in the (a) *x*-*y* plane and (b) the *x*-*z* plane. Filled black circles denote the positions of the oxygen on the carbonyl. The plots progress in pressure clockwise from the designating letters, (a) and (b), as 5, 35, 50 and 52 kPa. Both plots show the full pore dimension of 7.5 × 7.5 nm (width × height) for (a) and 7.5 × 5.0 nm for (b).

using two plots. The first, figure 11(a), is of the *x*-*y* plane of the simulation (top view of the surface) and the second, figure 11(b), is of the *x*-*z* plane (side view of the simulation box with the attractive surface at the bottom).

With figure 11 it can be seen that at 5 kPa, the adsorption is mostly about the carbonyls with only a single ammonia molecule at some distant point. At 35 kPa the number of molecules has increased with a few extra molecules about the carbonyls and with distant clusters and single ammonia molecules. The adsorption at this pressure still stays very much at the surface, even at the carbonyls. At 50 kPa the increase in the number of ammonia molecules has occurred by increasing the size of the clusters at the surface, including the cluster about the carbonyls. The clusters have grown to such an extent that they have started to join together. At 52 kPa the adsorption has suddenly increased in a condensation like manner. A dense monolayer has formed, with some space left for additional packing, together with the start of the second layer of adsorption. So in agreement with the distributions in figures 8 and 10, the adsorption up to 52 kPa is almost exclusively at the surface and with increasing association of ammonia molecules at the surface. Snapshots at the same pressures as figure 11 are presented in figure 12 for a simulation with no functional groups.

The configurations in figure 12 are very similar to those in figure 11 if the carbonyls and their associated cluster of ammonia molecules were removed. Ignoring what happens at the carbonyl groups, the mechanism of single molecule to cluster formation to cluster bridging is shared by both simulations. So the adsorption of additional molecules beyond any initial adsorption at functional groups is by the addition of molecules to two-dimensional ammonia clusters.

In addition to the effect of a single cluster, the effect of multiple clusters and many evenly distributed single carbonyls was investigated. The first of these presented are the isotherms for a surface with 0, 9, 25 and 49 evenly

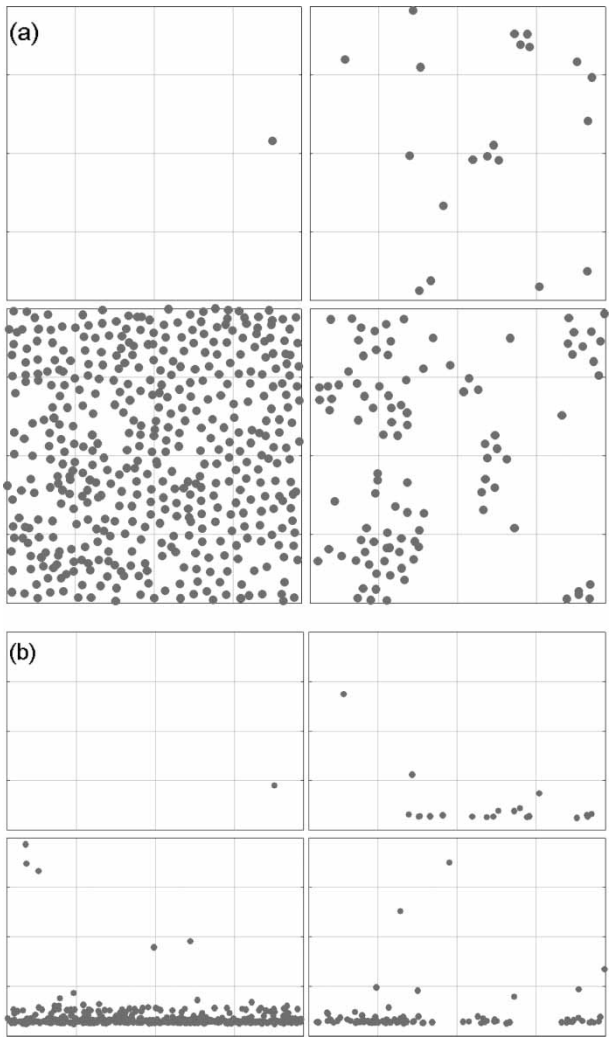

Figure 12. As per figure 11 but for a simulation with no carbonyls.

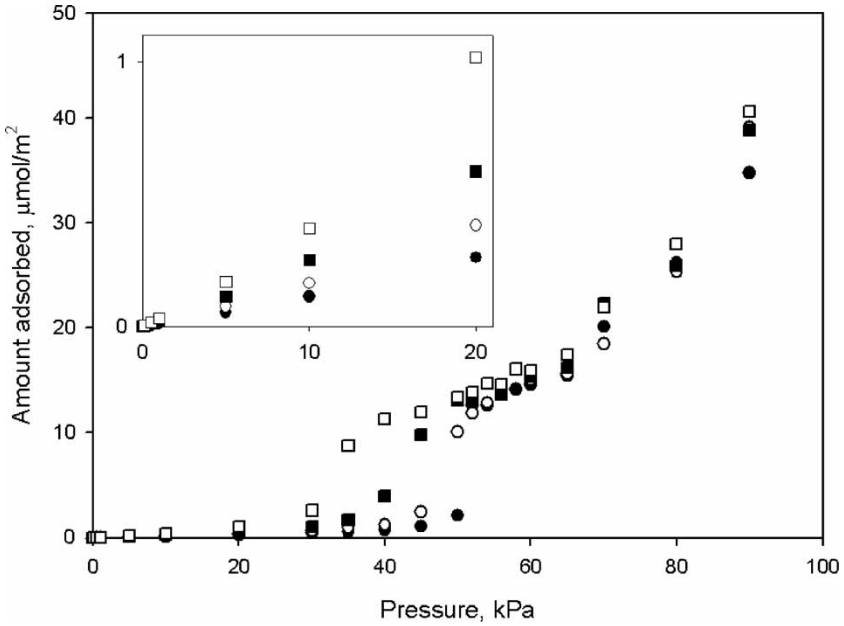

Figure 13. Simulation results for the adsorption of ammonia at 240 K on carbon black with zero (filled circles), 9 (empty circles), 25 (filled squares) and 49 (empty squares) evenly distributed single carbonyls. Inset graph is the same plot over the range of 0–21 kPa.

distributed single carbonyls (refer to figure 1(b) for configuration of carbonyls) in figure 13.

The increasing number of carbonyls increases the amount adsorbed significantly up to the monolayer condensation of the surface with no carbonyls at 52 kPa. The transition to monolayer coverage is changed significantly as the number of carbonyls is increased. The transition becomes smoother and the inflection point occurs at a lower pressure as the number of carbonyls is increased. From 52 kPa onwards the adsorption is qualitatively and quantitatively very similar for all configurations. The smoothing of the inflection point after monolayer coverage makes the adsorption isotherm more like the experimental results. However the movement of the transition to monolayer to a lower pressure further increases

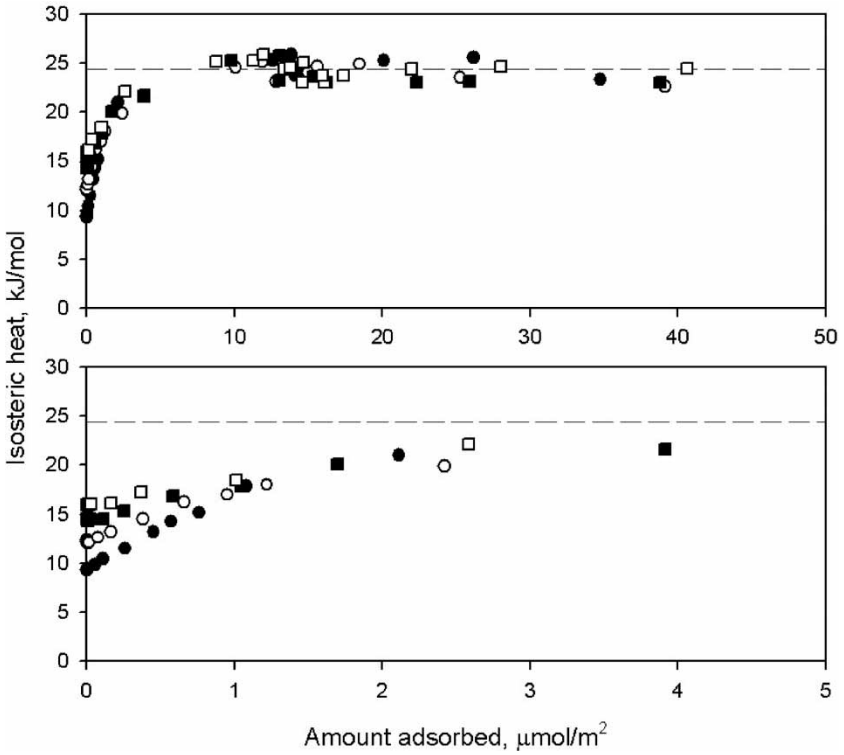

Figure 14. Isosteric heats of adsorption for ammonia on carbon black from simulation. Symbols have the same meaning as figure 13. The horizontal dashed lined corresponds to the heat of vaporisation for model ammonia from GEMC. Figures (a) and (b) differ only in the scale of the amount adsorbed.

the difference between the simulation and experiment results. The isosteric heats for the isotherms in figure 13 are shown in figure 14.

Figure 14 shows that the isosteric heats increase with increasing numbers of carbonyls. The increase in the isosteric heat is largest at low coverage with the isosteric heat of all configuration converging as the amount adsorbed increases. However, the increase in isosteric heat from the carbonyl free surface, even for a system of 49 carbonyls, is small compared with the increases seen in figure 5 for the addition of five closely grouped carbonyls. Certainly the isosteric heats are not close to having a similar shape to the experimental results in figure 7. By inspection of z-distributions and snapshots of simulations, the adsorption was found to occur by the two-dimensional clustering mechanism for all configurations of evenly distributed carbonyls. These plots are not shown here for brevity. The final carbonyl configurations considered are those with several groups of five carbonyls. In addition to the single group of five carbonyls already discussed, simulations were conducted with four and nine evenly spaced groups of five carbonyls (refer to figure 1(c)). All groups of five carbonyls discussed in the following results have a characteristic separation, δ, of 0.3 nm. The isotherms for the simulations with one, four and nine groups of five carbonyls are presented in figure 15.

The isotherms in figure 15 are similar to those in figure 13 with the increasing number of carbonyls increasing the amount adsorbed, smoothing the transition to monolayer coverage and lowering the pressure of the inflection point. Once the monolayer is formed, the adsorption of the different configurations is very similar. So by increasing the heterogeneity of the surface with more carbonyl groups, the shape of the isotherm becomes smoother after the inflection point like the experimental isotherm. However the shifting of the inflection point to lower pressure and a less sharp transition to monolayer coverage are in disagreement with experiment isotherms. The mechanism of adsorption remains the same as that previously discussed. The initial adsorption is always about the carbonyls followed by the two-dimensional clustering of the ammonia at the surface. As the number of groups of five carbonyls is increased, the distance that clusters have to bridge between clusters about the carbonyls is decreased. This causes the bridging of clusters, like that seen in figure 11(a) at 50 kPa, to occur at lower pressures. This causes the greater adsorption, prior to monolayer coverage, of the surfaces with four and nine groups of five carbonyls compared to the adsorption with just a single group. The isosteric heats for the isotherms in figure 15 are presented in figure 16.

The isosteric heats for all configurations in figure 16 retain the features of an initial isosteric heat greater than the heat of vaporisation, a minimum less than the heat of vaporisation and a subsequent increase in the isosteric heat. The isosteric heat at near zero adsorption is the same for all configurations suggesting that initially all groups act as independent sites for the adsorption. This is supported by the fact that up to 5 kPa, the amount adsorbed is proportional to the number of groups of five carbonyls. However there are two differences between the isosteric heat curves for a single group of five carbonyls and multiple groups. As the number of groups is increased, the minimum is shifted to higher loading, and the minimum has a higher value meaning that the curve becomes shallower about the minimum. These changes in the isosteric heat curves bring the simulation isosteric heats more in agreement with those from experiment in figure 7 and the results presented by Carman and Raal [15]. In figure 6 it was shown that the difference in isosteric heat

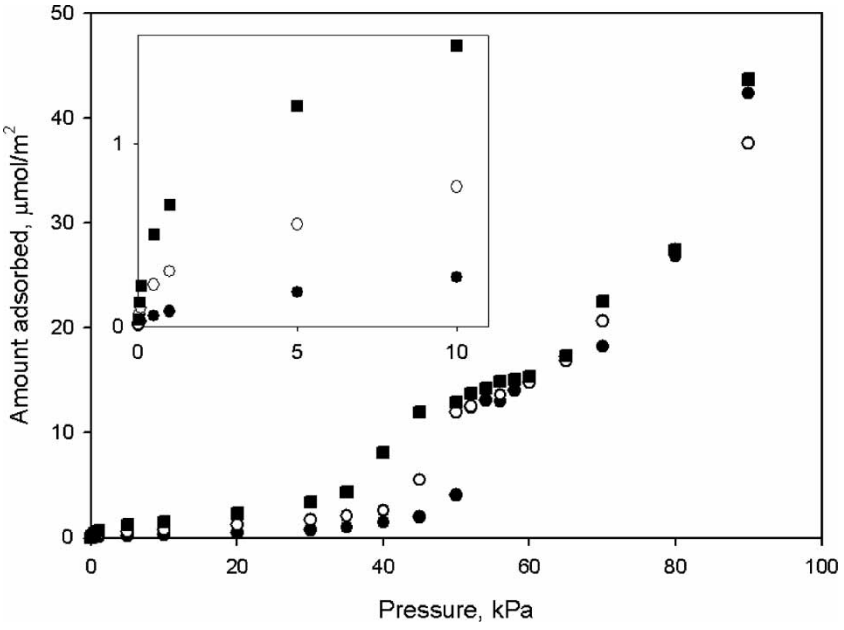

Figure 15. Simulation results for the adsorption of ammonia at 240 K on carbon black with one (filled circles), four (empty circles) and 9 (filled squares) groups of five carbonyls with $\delta = 0.3$ nm. Inset graph is the same plot over the range of 0–11 kPa.

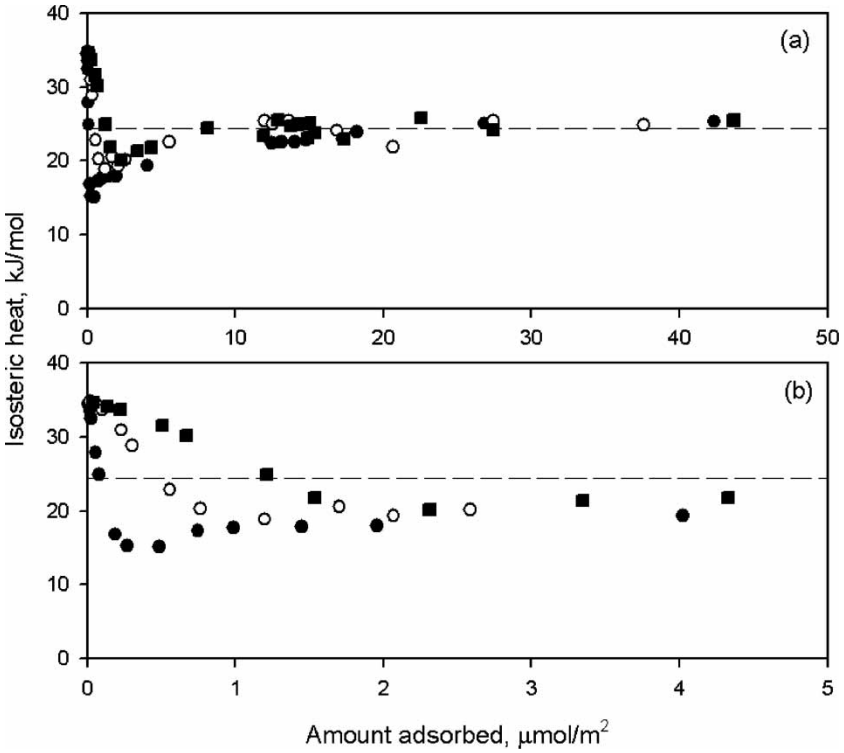

Figure 16. Isosteric heats of adsorption for ammonia on carbon black from simulation. Symbols have the same meaning as figure 15. The horizontal dashed lined corresponds to the heat of vaporisation for model ammonia from GEMC. Figures (a) and (b) differ only in the scale of the amount adsorbed.

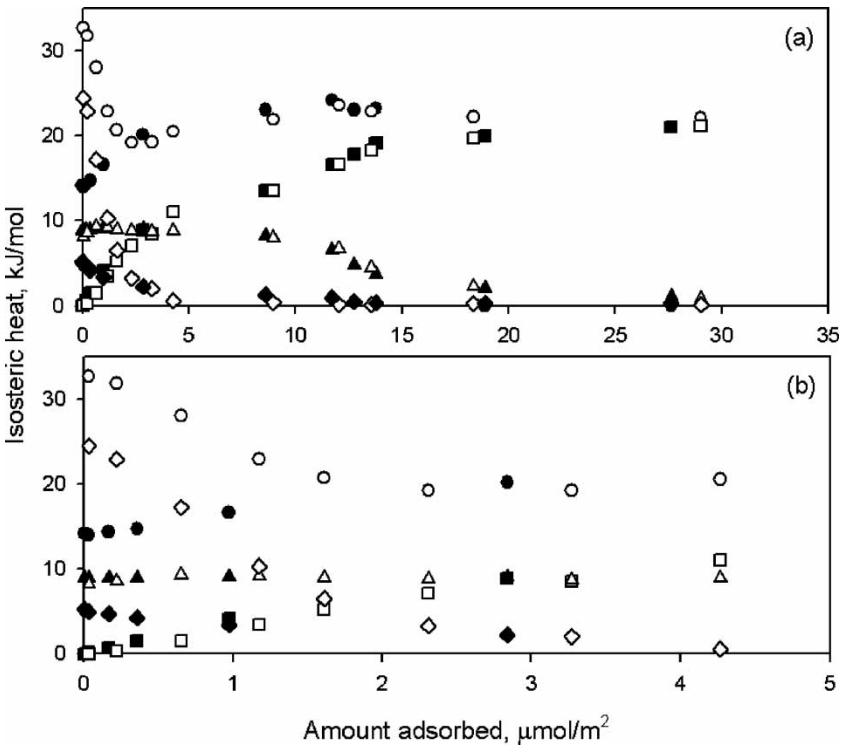

Figure 17. Simulation isosteric heats split into its contributions: total isosteric heat less the second term in equation 5 (circles), due to fluid–fluid interactions (squares), due to fluid solid interactions (triangles) and due to fluid-functional interactions (diamonds). Empty symbols denote the surface with 9 groups of five carbonyls with $\delta = 0.3$ nm and the filled symbols denote the surface with 49 evenly distributed carbonyls. Plots (a) and (b) differ only in the scale of the amount adsorbed.

between a surface with no carbonyls and one with five closely grouped carbonyls was due completely to the fluid-functional interactions. To see if this was also the case for higher concentrations of carbonyls, the contributions to the isosteric heat were plotted in figure 17.

Figure 17 shows that the difference in isosteric heat between the two configurations is mostly due to the carbonyls. The differences in the fluid–fluid and fluid–solid between the two are minimal. So even with a reasonable concentration of evenly distributed or grouped carbonyls, the mechanism remains the same for the two once the grouped carbonyls become saturated and adsorption continues at other points on the surface. So the addition of carbonyls improves the prediction of the isosteric heat against the experimental data but also causes the isotherm to become less like the experimental data. This suggests that increased heterogeneity is required to give the experimental isosteric heats observed. However using only carbonyls and the limited range of configurations studied here, it is not possible to satisfactorily reproduce the experimental data. Further studies would ideally require additional experimental data at different temperatures and particularly at higher temperatures than those studied by Spencer *et al.* [12] and Avgul and Kiselev [13]. A more complete simulation model would include aspect of surface of finite extent, additional functional groups and possibly pores.

5. Conclusions

Monte Carlo simulations have been performed using the grand canonical ensemble to study the adsorption of ammonia on graphitized carbon black at 240 K. The graphitized carbon black was modelled using the Steele potential for the carbon together with various arrangements of carbonyls. Simulation isotherms with low carbonyl concentrations showed a striking resemblance with available experimental isotherms for sub-critical ammonia on highly graphitized carbon black. For simulations with no carbonyls or with five located at the centre of the pore, initially low adsorption was followed by a sudden transition to approximately monolayer coverage. From the monolayer coverage, additional adsorption was by layering. The pressure at which the monolayer was formed was a point of inflection in the isotherm similar to that seen in experiments in the literature. However the isosteric heat from simulation was sometimes qualitatively completely different from experiment. A surface with no carbonyls or with five carbonyls separated by more than 0.6 nm gave isosteric heats initially less than the heat of vaporisation and only approached the heat of vaporisation at high coverage once a monolayer had been formed. A single group of five carbonyls separated by 0.15 or 0.3 nm gave isosteric heats which matched experiment more closely with an isosteric heat greater than the heat of vaporisation initially, followed by a minimum less than the isosteric heat before increasing again to be equal to the heat of vaporisation beyond monolayer coverage. Beyond monolayer coverage both the isotherms and the isosteric heats were similar for all configurations. The mechanism of adsorption, prior to the formation of the monolayer, was exhaustively shown to be two-dimensional clustering of the ammonia molecules. If carbonyls were present, this is where the clustering would initially begin. However as the pressure was increased clustering would occur not only around the carbonyls but also at distant points on the surface. This meant that once the carbonyls were saturated with ammonia, the mechanism of adsorption for surfaces with and without carbonyls was identical. The effect of increasing heterogeneity was investigated with evenly distributed single carbonyls and evenly distributed groups of five carbonyls. It was found that increasing the number of carbonyls by either method decreased the sharpness of the transition to monolayer coverage and decreased the pressure of the inflection point. The effect on isosteric heat by evenly distributed carbonyls was minimal, meaning that this type of configuration did not reflect the isosteric heats seen in the literature. Increasing the number of groups of five carbonyls had the effect of increasing the minimum in the isosteric heat, increasing the pressure at which the minimum occurred and caused the curve to become shallower about the minimum. This was more in agreement with the isosteric heats seen in the literature.

So a simple model of carbon black involving a Steele potential surface and several carbonyls is able to reproduce many essential features of ammonia adsorption on graphitized carbon black. However this can only be considered an initial study with many other factors possibly having an effect on the results presented. These may include (not exhaustively) other types of functional groups, small numbers of pores and finite size effects. These effects may be separable using ammonia with its strong association with itself and moderate association with the carbon surface. This would be the focus of future studies in this area.

Acknowledgements

This research was made possible by the Australian Research Council whose support is gratefully acknowledged. Thanks also to the University of Queensland High Performance Computing facility for a generous allocation of computing time.

References

[1] N. Metropolis, A.W. Rosenbluth, M.N. Rosenbluth, A.H. Teller, E. Teller. Equation-of-state calculations by fast computing machines. *J. Chem. Phys.*, **21**, 1087 (1953).

[2] T. Kristof, J. Vorholz, J. Liszi, B. Rumpf, G. Maurer. A simple effective pair potential for the molecular simulation of the thermodynamic properties of ammonia. *Mol. Phys.*, **97**(10), 1129 (1999).

[3] A.Z. Panagiotopoulos. Direct determination of phase coexistence properties of fluids by Monte Carlo simulation in a new ensemble. *Mol. Phys.*, **61**(4), 813 (1987).

[4] W.A. Steele. Physical interaction of gases with crystalline solids. I. Gas-solid energies and properties of isolated adsorbed atoms. *Surf. Sci.*, **36**(1), 317 (1973).
[5] M. Jorge, N.A. Seaton. Molecular simulation of phase coexistence in adsorption in porous solids. *Mol. Phys.*, **100**(24), 3803 (2002).
[6] W.L. Jorgensen, J. Tirado-Rives. The OPLS (optimized potentials for liquid simulations) potential functions for proteins, energy minimizations for crystals of cyclic peptides and crambin. *J. Am. Chem. Soc.*, **110**(6), 1657 (1988).
[7] M. Jorge, C. Schumacher, N.A. Seaton. Simulation study of the effect of the chemical heterogeneity of activated carbon on water adsorption. *Langmuir*, **18**(24), 9296 (2002).
[8] T. Morimoto, K. Miura. Adsorption sites for water on graphite. 1. Effect of high-temperature treatment of sample. *Langmuir*, **1**(6), 658 (1985).
[9] T. Morimoto, K Miura. Adsorption sites for water on graphite. 2. Effect of autoclave treatment of sample. *Langmuir*, **2**(1), 43 (1986).
[10] M.P. Allen, T.P. Tildesley. *Computer Simulation of Liquids*, Clarendon Press, Oxford (1987).
[11] D. Nicholson, N.G. Parsonage. *Computer Simulation and the Statistical Mechanics of Adsorption*, Academic Press, London (1982).
[12] W.B. Spencer, C.H. Amberg, R.A. Beebe. Further studies of adsorption on graphitized carbon blacks. *J. Phys. Chem.*, **62**, 719 (1958).
[13] N.N. Avgul, A.V. Kiselev. Physical adsorption of gases and vapors on graphitized carbon blacks. *Chem. Phys. Carbon*, **6**, 1 (1970).
[14] R.M. Dell, R.A. Beebe. Heats of adsorption of polar molecules on carbon surfaces. II. Ammonia and methylamine. *J. Phys. Chem.*, **59**, 754 (1955).
[15] P.C. Carman, F.A. Raal. Monolayer capacities in multilayer adsorption. *T. Faraday Soc.*, **49**, 1465 (1953).